Stability and bifurcation analysis of a two-degree-of-freedom system with clearances

N. Kranjcevic, M. Stegic*, N. Vrankovic

University of Zagreb, Faculty of Mechanical Engineering and Naval Architecture, Zagreb 10002, Croatia

Abstract

The time finite element method is used in this paper for the stability and bifurcation analysis of a two-degree-of-freedom system with clearances under periodic excitations. The analysis is based on the utilization of the Poincare map in which the stability of a periodic solution is transformed to that of a fixed point.

Keywords: Nonlinear vibrations; Clearances; Stability; Neimark bifurcation

1. Introduction

Clearances exist in many mechanical systems either by design or due to the manufacturing tolerances and wear. Vibrations of such systems can result in relative motion across the clearance space and impacting between the components.

The governing equations of motion include abrupt variation of stiffness which can be assumed as piecewise linear. A complete characterization of the dynamic behaviour of piecewise linear systems requires, among other things, determination of stability of their steady state solutions. Delineation of the stable and unstable solutions could help in predicting their periodic, quasi-periodic and chaotic motions and transitions to either type of response.

In this paper, the mechanical system with clearances is considered. The time finite element method is used to obtain the steady state solutions while the stability and bifurcation analysis is performed by using Poincare map.

2. Problem formulation

The mechanical model of a three-degree-of-freedom semi-definite system with clearances consists of three mass elements, two linear viscous dampers, and two clearance type nonlinearities $h(q_1)$, $h(q_2)$. With $\boldsymbol{q}^T = [q_1, q_2]$ being the nondimensional displacement, the equation of motion can be expressed as:

$$\boldsymbol{q}'' + \boldsymbol{Z}\boldsymbol{q}' + \boldsymbol{\Omega}\boldsymbol{h}(\boldsymbol{q}) = \boldsymbol{f}_0 + \boldsymbol{f}_a \cos(\eta\tau) \tag{1}$$

where:

$$\boldsymbol{Z} = 2\begin{bmatrix} \zeta_{11} & -\zeta_{12}\omega_{12} \\ -\zeta_{21}\omega_{21} & \zeta_{22}\omega_{22} \end{bmatrix}, \ \boldsymbol{\Omega} = \begin{bmatrix} 1 & -\omega_{12}^2 \\ -\omega_{21}^2 & \omega_{22}^2 \end{bmatrix},$$
$$\boldsymbol{h}^T(\boldsymbol{q}) = [\,h(q_1), \quad h(q_2)\,] \tag{2}$$

Furthermore, $(\cdot)'$ denotes $\frac{\mathrm{d}(\cdot)}{\mathrm{d}\tau}$, τ is the normalized time, η denotes the nondimensional excitation frequency while $\boldsymbol{f}_o$ and $\boldsymbol{f}_a$ are the amplitude vectors of mean and alternating load, respectively.

Exact solutions of piecewise linear equations of motion are very rare and almost all of the methods for their solving are only approximate. Commonly used solution methods are the classical numerical time integration (Runge–Kutta, etc.), the harmonic balance method, the incremental harmonic balance method, the piecewise full decoupling method [1] and the time finite element method [2].

3. The time finite element method

The time finite element method will be applied for solving Eq. (1). Using Hamilton weak principle, the basic equation which describes the motion of the mechanical system with clearances between the two known times τ_1 and τ_2 is:

* Corresponding author. Tel.: +385 161 68135; Fax: +385 161 68187; E-mail: mstegic@fsb.hr

Computational Fluid and Solid Mechanics 2005
K.J. Bathe (Editor)

$$\int_{\tau_1}^{\tau_2} \left\{ \delta \boldsymbol{q}'^T \boldsymbol{q}' + \delta \boldsymbol{q}^T \left[-\boldsymbol{Z}\boldsymbol{q}' - \boldsymbol{\Omega} \boldsymbol{h}(\boldsymbol{q}) + \boldsymbol{f}_0 + \boldsymbol{f}_a \cos(\eta\tau) \right] \right\} \mathrm{d}\tau = \delta \boldsymbol{q}^{\mathrm{T}} \boldsymbol{p} \Big|_{\tau_1}^{\tau_2} \quad (3)$$

where $\boldsymbol{p}$ is the vector of the generalized momenta. The basis of the finite element in time approximation is, the division of the time interval $\tau_2 - \tau_1$ equals the period of excitations, into a finite number n_e of time elements. Similar to the standard finite element technique, the displacement $\boldsymbol{q}_j$ within each time element is interpolated among their respective nodal variables $\bar{\boldsymbol{q}}_j$ by using the standard shape functions $\boldsymbol{N}_j$.

Inserting the finite element interpolation into Eq. (3), the following finite element equation at the time element level is obtained:

$$\boldsymbol{A}_j \, \bar{\boldsymbol{q}}_j + \boldsymbol{g}_j(\bar{\boldsymbol{q}}_j) + \boldsymbol{f}_j = \boldsymbol{p}_j, \quad j = 1(1)n_e \quad (4)$$

where:

$$\boldsymbol{A}_j = \int_{\tau_j}^{\tau_{j+1}} [\boldsymbol{N}_j'^T \boldsymbol{N}_j' - \boldsymbol{N}_j^T \, Z \boldsymbol{N}_j'] \mathrm{d}\tau \quad (5)$$

$$\boldsymbol{g}_j(\bar{\boldsymbol{q}}_j) = -\int_{\tau_j}^{\tau_{j+1}} \boldsymbol{N}_j^T \, \boldsymbol{\Omega} \boldsymbol{h}(\boldsymbol{q}) \mathbf{d}\boldsymbol{\tau} \quad (6)$$

$$\boldsymbol{f}_j = \int_{\tau_j}^{\tau_{j+1}} [\boldsymbol{N}_j^T \boldsymbol{f}_0 + \boldsymbol{N}_j^T \boldsymbol{f}_a \cos(\eta\tau)] \mathrm{d}\tau \quad (7)$$

The global finite element equation can be determined by assembling the finite element equation as at the time element level (4), as in the standard finite element modelling scheme, yielding

$$\boldsymbol{A}\bar{\boldsymbol{q}} + \boldsymbol{g}(\bar{\boldsymbol{q}}_j) + \boldsymbol{f} = 0 \quad (8)$$

Thus, Eq. (8) results in a set of nonlinear algebraic equations in unknown nodal displacement $\bar{\boldsymbol{q}}$. Using the Newton–Raphson numerical method, the nodal displacement $\bar{\boldsymbol{q}}$ may be expressed in an iteration procedure as:

$$\bar{\boldsymbol{q}}^{(n+1)} = \bar{\boldsymbol{q}}^{(n)} + \Delta \bar{\boldsymbol{q}}^{(n)} \quad (9)$$

For a small increment $\Delta \bar{\boldsymbol{q}}^{(n)}$, Eq. (8), can be expanded into the Taylor series retaining only the linear terms:

$$\boldsymbol{d}^{(n)} + \boldsymbol{K}^{(n)} \, \Delta \bar{\boldsymbol{q}}^{(n)} = 0 \quad (10)$$

where:

$$\boldsymbol{d}^{(n)} = \boldsymbol{A}^{(n)} \bar{\boldsymbol{q}}^{(n)} + \boldsymbol{g}^{(n)}(\bar{\boldsymbol{q}}) + \boldsymbol{f} \quad (11)$$

$$\boldsymbol{K}^{(n)} = \boldsymbol{A}^{(n)} + \frac{\partial \boldsymbol{g}^{(n)}(\bar{\boldsymbol{q}})}{\partial \bar{\boldsymbol{q}}^{(n)}} \quad (12)$$

The iteration procedure requires evaluation of the components of vector $\boldsymbol{d}^{(n)}$ and tangent matrix $\boldsymbol{K}^{(n)}$ at each iteration step. The components of matrix $\boldsymbol{A}$ and vector $\boldsymbol{f}$ are constants and they need to be calculated only once. The numerical procedure will be terminated when the increment of nodal displacement $\Delta \bar{\boldsymbol{q}}$ converges towards zero.

4. Stability analysis by Poincare maps

The stability of the time finite element solutions is investigated as the stability of the Poincare map. Before using the Poincare map, a Poincare section has to be constructed. Points on a Poincare section can be determined considering a standard procedure of static condensation of time elements. It is briefly discussed as follows. Eq. (10), at the time element level, can be partitioned as:

$$\begin{bmatrix} \boldsymbol{d}_B \\ \boldsymbol{d}_I \end{bmatrix}_j + \begin{bmatrix} \boldsymbol{K}_{BB} & \boldsymbol{K}_{BI} \\ \boldsymbol{K}_{IB} & \boldsymbol{K}_{II} \end{bmatrix}_j \begin{bmatrix} \Delta \bar{\boldsymbol{q}}_B \\ \Delta \bar{\boldsymbol{q}}_I \end{bmatrix}_j = \begin{bmatrix} \boldsymbol{p}_B \\ 0 \end{bmatrix}_j, \quad j = 1(1)n_e \quad (13)$$

where B and I correspond the temporal nodes at the ends and in the interior of time element, respectively, while $\boldsymbol{p}_B$ denotes the vector of momenta at the boundary nodes. Substituting the lower part into the upper part of Eq. (13), we can eliminate the interior nodal displacement $\Delta \bar{\boldsymbol{q}}_{I\,j}$. Considering the assemblage procedure, $\Delta \bar{\boldsymbol{q}}_{B\,j}$ of all time elements are further condensed by imposing the compatibility conditions at the common node of the two elements, yielding the elimination of the common node. This procedure results into the global equation:

$$\begin{bmatrix} \boldsymbol{d}_1 \\ \boldsymbol{d}_2 \end{bmatrix} + \begin{bmatrix} \boldsymbol{K}_{11} & \boldsymbol{K}_{12} \\ \boldsymbol{K}_{21} & \boldsymbol{K}_{22} \end{bmatrix} \begin{bmatrix} \Delta \bar{\boldsymbol{q}}_1 \\ \Delta \bar{\boldsymbol{q}}_2 \end{bmatrix} = \begin{bmatrix} -\boldsymbol{p}_1 \\ \boldsymbol{p}_2 \end{bmatrix} \quad (14)$$

where 1 and 2 denote the initial and final time nodes. If $\eta^{\mathrm{T}} = [\Delta \bar{\boldsymbol{q}}, \boldsymbol{p}]$ represents a point on the Poincare section, Eq. (14) can be modified as the relationship between two fixed points:

$$\begin{bmatrix} \Delta \bar{\boldsymbol{q}}_2 \\ \boldsymbol{p}_2 \end{bmatrix} = \begin{bmatrix} & -\boldsymbol{K}_{12}^{-1} \boldsymbol{K}_{11} & -\boldsymbol{K}_{12}^{-1} \\ \boldsymbol{K}_{21} & -\boldsymbol{K}_{22} \boldsymbol{K}_{12}^{-1} \boldsymbol{K}_{11} & -\boldsymbol{K}_{22} \boldsymbol{K}_{12}^{-1} \end{bmatrix} \begin{bmatrix} \Delta \bar{\boldsymbol{q}}_1 \\ \boldsymbol{p}_1 \end{bmatrix} + \begin{bmatrix} -\boldsymbol{K}_{12}^{-1} & 0 \\ -\boldsymbol{K}_{22} \boldsymbol{K}_{12}^{-1} & \boldsymbol{I} \end{bmatrix} \begin{bmatrix} \boldsymbol{d}_1 \\ \boldsymbol{d}_2 \end{bmatrix} \quad (15)$$

The Poincare map $\boldsymbol{P}$ is defined by:

$$\boldsymbol{P}(\boldsymbol{\eta}) = \boldsymbol{x}(\boldsymbol{\eta}, \boldsymbol{\tau}_1, \boldsymbol{\tau}_2) = \boldsymbol{\eta} \quad (16)$$

In a neighborhood of the fixed point of the map, we have

$$\boldsymbol{P}(\boldsymbol{\eta} + \boldsymbol{v}) = \boldsymbol{P}(\boldsymbol{\eta}) + \frac{\partial \boldsymbol{P}}{\partial \boldsymbol{\eta}} \boldsymbol{v} + \boldsymbol{O}(\| \boldsymbol{v}^2 \|) \qquad (17)$$

where $\|\boldsymbol{v}\|$ is the norm of the deviation from the fixed point on the Poincare section. Information on the stability of the fixed point $\boldsymbol{\eta}$ can be obtained by studying the eigenvalues of the Jacobian matrix $\partial \boldsymbol{P}/\partial \boldsymbol{\eta}$. If the eigenvalues are inside the unit circle the system is asymptotically stable; if at least one of the eigenvalues is outside the circle the system is unstable. The stability boundary is the unit circle itself. If the eigenvalues are real there are only two points at which they can cross the stability boundary, $\Phi = 0, \pi$. If the eigenvalues are complex conjugate they can cross the unit circle at an angle $\Phi \neq 0, \pi$ and this is so-called Neimark instability.

5. Results

The frequency responses of a three-degree-of-freedom semi-definite dynamical system with two clearances are calculated here using the time finite element method. The system parameters $\zeta_{11} = \zeta_{12} = \zeta_{21} = \zeta_{22} = 0.05$, $\omega_{12} = \omega_{21} = 0.6$, $\omega_{22} = 1.1$, $\boldsymbol{f}_0^T = [0.5, 0.25]$ and $\boldsymbol{f}_a^T = [0.25, 0]$ are adopted from Padmanbhan et al. [3] where the system with one clearance was studied by using the harmonic balance method.

The time finite element method cannot solve problems with ideal clearance because the zero stiffness implies the singularity of the tangent matrix $\boldsymbol{K}^{(n)}$. In the finite element calculations, the clearance nonlinearity $h(q_i)$ is approximated by the trilinear system at which the slope of the second stage is 1% of the slope of the first and third stage. Furthermore, the finite element calculations were performed with ten four-node time elements and with the iteration procedure limited on 100 iterations.

Considering the response of the linear system as the starting vector, the frequency response, in terms of the nondimensional excitation frequency η and the steady state amplitude $\hat{q}_1$, is obtained and presented in Fig. 1. As the result of computations, the unconverged or unstable solutions are obtained in the interval of $0.7 < \eta < 0.96$. Using the previous stable solution as the starting vector, only the unstable solutions are found within narrow bounds $0.77 < \eta < 0.94$ (Fig. 2).

Imposing small increments in the excitation frequency, the points where the eigenvalues of the Jacobian matrix cross the unit circle can be determined. For the excitation frequency $\eta = 0.772$, the eigenvalues are:

$$\begin{aligned} \lambda_{1,2} &= -0.0527 \pm 0.9939i, \qquad |\lambda_{1,2}| = 0.9953 \\ \lambda_{3,4} &= 0.0266 \pm 0.4267i, \qquad |\lambda_{3,4}| = 0.4275 \end{aligned} \qquad (18)$$

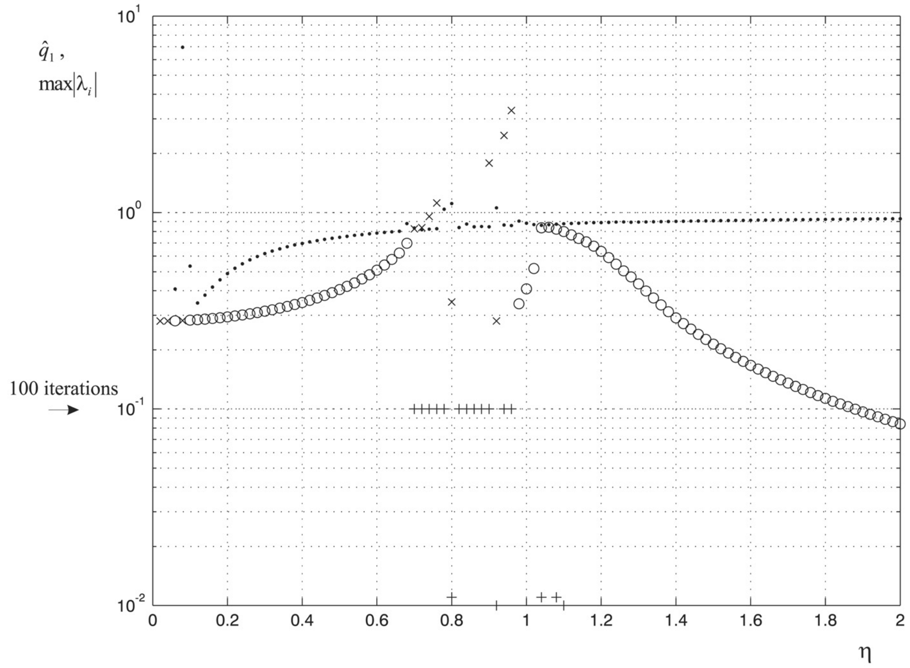

Fig. 1. Frequency response of the three-degree-of-freedom semi-definite system with clearances: o – asymptotically stable, x – unstable or achieved maximum of 100 iterations, + number of iterations/100, ● max $|\lambda i|$.

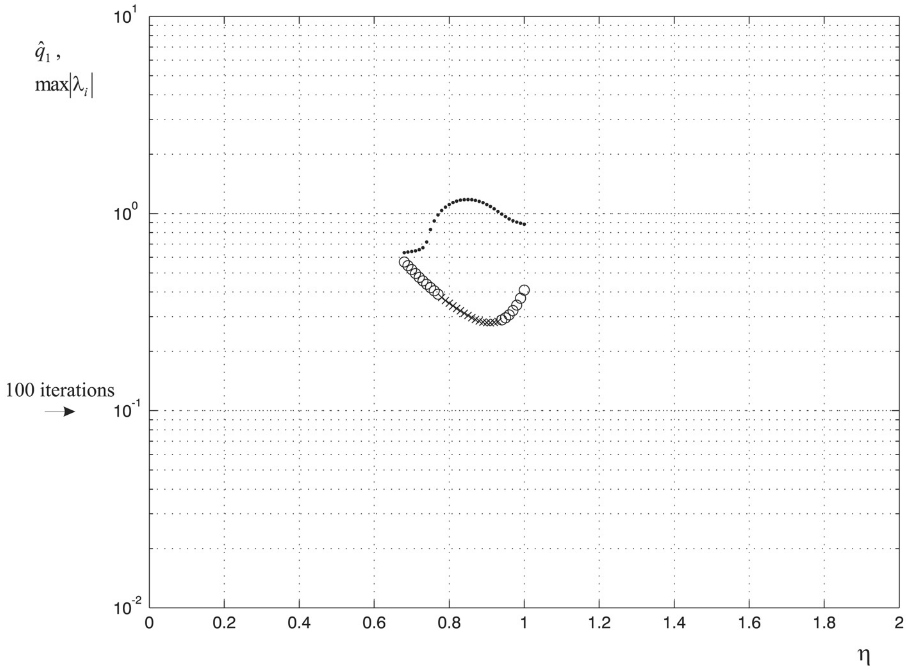

Fig. 2. Frequency response of the three-degree-of-freedom semi-definite system with clearances: o – asymptotically stable, x – unstable, + number of iterations/100, • max$|\lambda i|$.

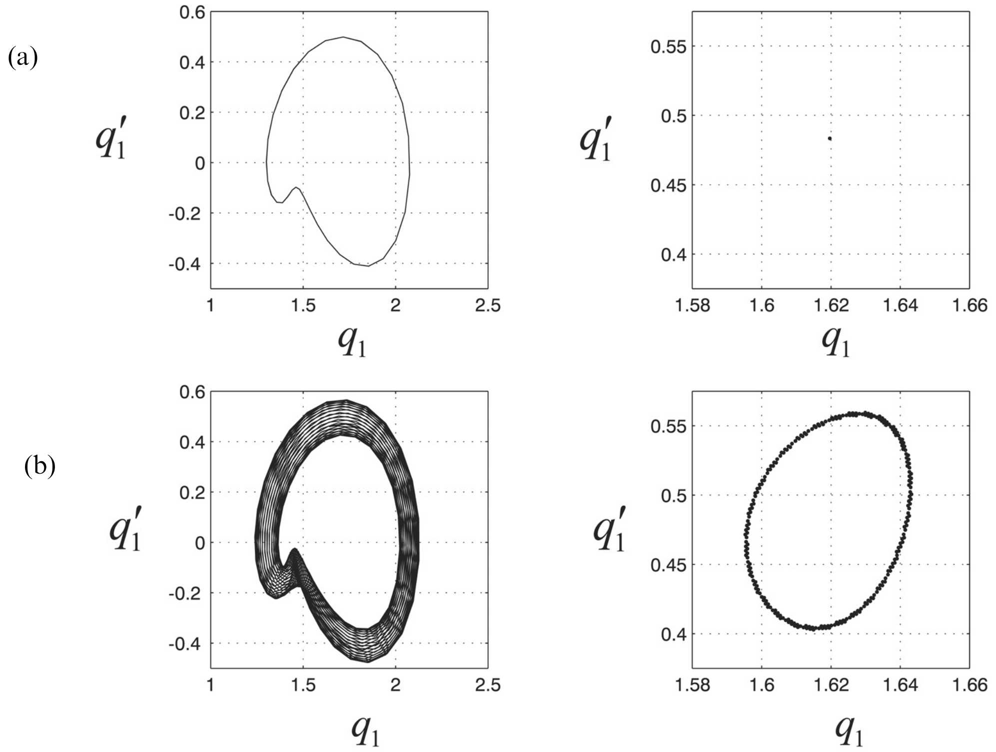

Fig. 3. Phase portraits and Poincare sections showing the Neimark bifurcation: a) $\eta = 0.772$, b) $\eta = 0.773$.

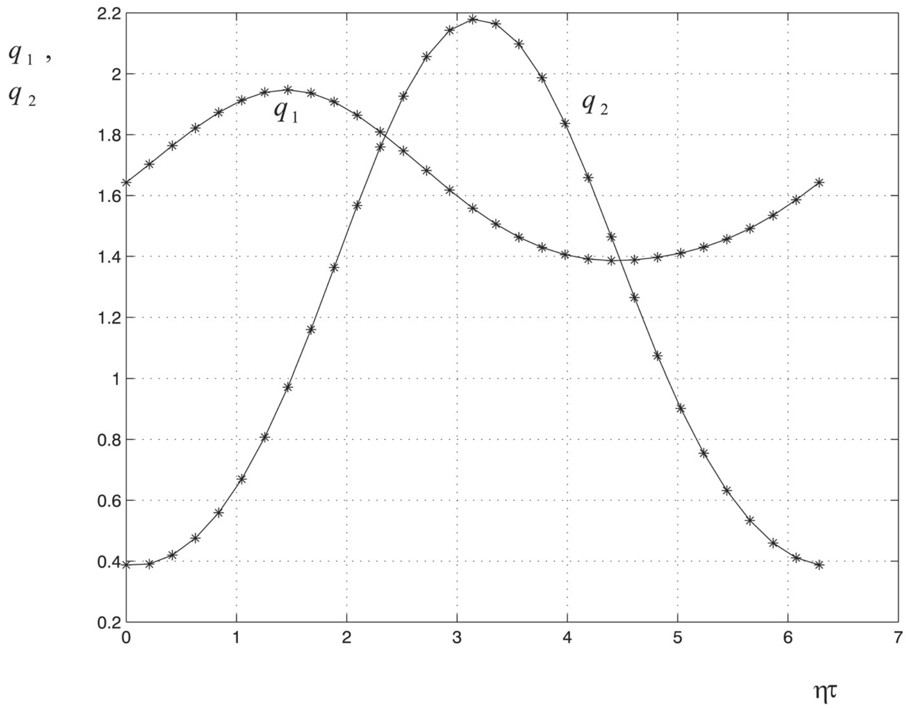

Fig. 4. The unstable periodic solutions $q_1(\tau)$ and $q_2(\tau)$ for $\eta = 0.92$.

(asymptotically stable solution), while the excitation frequency $\eta = 0.773$ generates:

$$\begin{aligned} \lambda_{1,2} &= -0.0496 \pm 0.9996i, \qquad |\lambda_{1,2}| = 1.0008 \\ \lambda_{3,4} &= 0.028 \pm 0.4247i, \qquad |\lambda_{3,4}| = 0.4256 \end{aligned} \tag{19}$$

(unstable solution). These results indicate that a complex conjugate pair of the eigenvalues crosses the unit circle away from the real axis resulting in Neimark bifurcation. The branch of stable periodic solution, that exists prior to the bifurcation, continues as a branch of unstable periodic or two period quasiperiodic solutions, after the bifurcation. The qualitatively different phase portraits (Fig. 3) confirm the Neimark bifurcation.

In the range of unstable solutions exist two unstable periodic solutions ($\eta = 0.80$ and $\eta = 0.92$), see Fig. 4; other solutions are quasiperiodic.

6. Conclusions

The time finite element method is an implicit method that gives accurate numerical results with only few time elements and without significant computational efforts. The stability and bifurcation analysis can be performed by investigating the eigenvalues of the Jacobian matrix which is a by-product of finite element procedure.

References

[1] Kranjcevic N, Stegic M, Vrankovic N. The piecewise full decoupling method for vibrating systems with clearances. In: Eberhardsteiner J, Mang HA, editors. Proceedings of WCCM-V. Vienna: Vienna University of Technology, 2002.

[2] Wang Y. Dynamics of unsymmetric piecewise-linear/non-linear systems using finite elements in time. J of Sound and Vibration 1995;185:155–170.

[3] Padmanabhan C, Singh R. Spectral coupling issues in a two-degree-of-freedom system with clearance non-linearities. J of Sound and Vibration 1992;155:209–230.

[4] Nayfeh AH, Balachandran B. Applied nonlinear dynamics. John Wiley & Sons: New York, 1995.